JACS
JOURNAL OF THE AMERICAN CHEMICAL SOCIETY
Article
pubs.acs.org/JACS

The Highly Reactive Benzhydryl Cation Isolated and Stabilized in Water Ice

Paolo Costa,[†] Miguel Fernandez-Oliva,[‡] Elsa Sanchez-Garcia,*[,‡] and Wolfram Sander*[,†]

[†]Lehrstuhl für Organische Chemie II, Ruhr-Universität Bochum, 44780 Bochum, Germany
[‡]Max-Planck-Institut für Kohlenforschung, 45470 Mülheim an der Ruhr, Germany

Supporting Information

ABSTRACT: Diphenylcarbene (DPC) shows a triplet ground-state lying approximately 3 kcal/mol below the lowest singlet state. Under the conditions of matrix isolation at 25 K, DPC reacts with single water molecules embedded in solid argon and switches its ground state from triplet to singlet by forming a strong hydrogen bond. The complex between DPC and water is only metastable, and even at 3 K the carbene center slowly inserts into the OH bond of water to form benzhydryl alcohol via quantum chemical tunneling. Surprisingly, if DPC is generated in amorphous water ice at 3 K, it is protonated instantaneously to give the benzhydryl cation. Under these conditions, the benzhydryl cation is stable, and warming to temperatures above 50 K is required to produce benzhydryl alcohol. Thus, for the first time, a highly electrophilic and extremely reactive secondary carbenium ion can be isolated in a neutral, nucleophilic environment avoiding superacidic conditions.

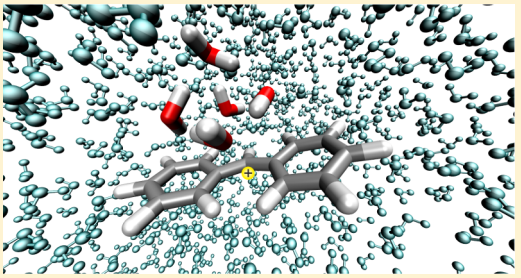

INTRODUCTION

Carbenium ions are among the most important reactive intermediates in chemistry. They play key roles in a very large number of reactions in the laboratory and in industrial chemical production.[1,2] The electrophilicity, and thus the reactivity, of carbenium ions stretches over many orders of magnitude, depending on the substituents at the positively charged carbon atom.[3−6] The benzhydryl cation **2** is a prototype of a strongly electrophilic secondary cation that in nucleophilic solvents, such as alcohols, is extremely short-lived (lifetimes in the order of picoseconds).[7] Only in superacidic, non-nucleophilic solvents, cation **2** is stable enough for spectroscopic characterization. Thus, in concentrated sulfuric acid, benzhydryl alcohol **3** is protonated and water eliminated to form a yellow solution of **2** with an absorption maximum at 442 nm.[8] The pK_R^+ value of **3** in sulfuric acid was determined to −13.3, which reveals the high electrophilicity of **2**, and explains its extremely short lifetime in nucleophilic solvents. Therefore, the spectroscopic characterization of **2** and related cations requires either superacidic solvents or ultrafast time-resolved techniques.

The most general route to **2** and related carbenium ions is the heterolysis of a C−X bond in a benzhydryl derivative or proton transfer to a singlet carbene such as diphenylcarbene S-**1**. Evidence that methanol is able to efficiently protonate carbene **1** was presented by Kirmse et al. more than 50 years ago.[9,10] Later, Kirmse, Kilian, and Steenken were able to provide spectroscopic evidence for the formation of **2** by protonation of **1** using picosecond UV−vis absorption spectroscopy.[11]

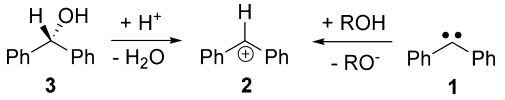

Kohler et al. investigated the protonation of **1** using femtosecond absorption spectroscopy.[7] In acetonitrile and cyclohexane, a transient species with an absorption maximum at 370 nm was assigned to singlet carbene S-**1**. The intersystem crossing (ISC) rates for the formation of triplet T-**1** was determined to 340 ps in acetonitrile and to 110 ps in cyclohexane, in excellent agreement with previous measurements by Eisenthal et al. using picosecond laser-induced fluorescence.[12,13] In neat methanol, S-**1** is protonated on an ultrafast time scale, and **2** is formed with a time constant of only 9 ps.[7] This is the fastest known intermolecular proton transfer to a carbon atom. Under these conditions, cation **2** is very short-lived and decays with a time constant of 31 ps by reaction with one of the surrounding methanol molecules.

Recently, we described the reaction of triplet T-**1** with single molecules of CH_3OH in argon matrices doped with 0.5−1% of methanol.[14] The singlet state S-**1** is highly basic and forms a very strong hydrogen bond with methanol, while T-**1**, similar to doublet radicals,[15−18] is only a weak hydrogen-bond acceptor. Since the stabilization of S-**1** compared to T-**1** in the methanol complex is larger than the S−T gap in **1**, the spin ground state of the carbene−methanol complex is shifted from triplet to singlet. Consequently, the singlet carbene complex S-**1**···$HOCH_3$ is formed. This complex is metastable and even at 3

Received: August 1, 2014
Published: September 7, 2014

dx.doi.org/10.1021/ja507894x | J. Am. Chem. Soc. 2014, 136, 15625−15630

K slowly reacts to ether **4**, the formal product of the OH-insertion, via quantum chemical tunneling (QMT).

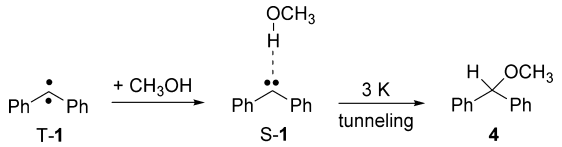

To explore the scope of this solvent-induced spin-flip, we investigated the reaction of **1** with water under similar conditions. In addition, we generated **1** in amorphous water ice at cryogenic temperatures. To our surprise, amorphous water ice is not only able to protonate **1** at temperatures as low as 3 K but also to kinetically stabilize the benzhydryl cation **2** and to suppress ion pair recombination. For the first time, a highly electrophilic and extremely reactive secondary carbenium ion can be isolated in a neutral, nucleophilic environment avoiding superacidic media.

RESULTS AND DISCUSSIONS

Reaction of DPC with Single Water Molecules. Triplet carbene T-**1** is obtained by photolysis of diphenyldiazomethane (DPDM) matrix isolated in argon doped with 0.5−1% water at 3 K. The IR spectrum of such a matrix shows the expected absorptions of water and of triplet carbene T-**1**, while reaction products are not observed. If such a matrix is annealed for several minutes at 25 K, water is diffusing and can now interact with the carbene. This results in the formation of a strongly hydrogen-bonded complex between the singlet carbene S-**1** and one water molecule (Scheme 1, Figure 1). The IR bands of S-**1**

Scheme 1. Reaction of Diphenylcarbene 1 with Water

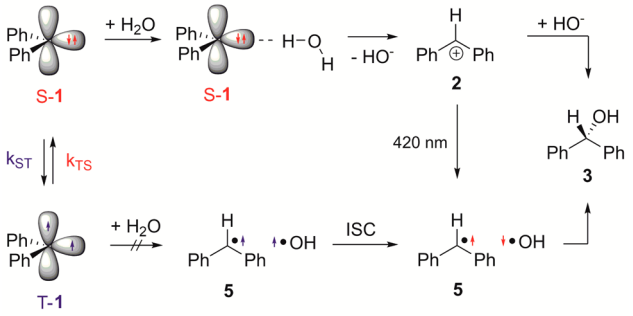

in the water complex are identical to that of the methanol complex described previously.[14] The strongest band of S-**1** at 1327.8 cm^{-1} is assigned to the asym. C−C−C str. vibration of the carbene center. On ^{13}C labeling of the carbene center, this band is red-shifted by −21.9 cm^{-1}, in agreement with predictions from DFT calculations (see Figure S5a).

The UV−vis spectra also show the formation of the singlet carbene S-**1** on annealing of a 1% water-doped argon matrix containing the triplet carbene T-**1** at 25 K: the characteristic absorption of T-**1** in the visible region (λ_{max} = 457 nm) strongly decreases in intensity, and a new UV band with λ_{max} = 360 nm appears simultaneously (Figure S6). This is in good agreement with the observation of a transient band with λ_{max} = 370 nm (in acetonitrile or cyclohexane as solvent) assigned to S-**1** by Kohler et al. using femtosecond transient absorption spectroscopy.[7]

These findings are corroborated by DFT calculations (BLYP-D3/def2-TZVP) of **1** and the **1**···H_2O complexes in the gas

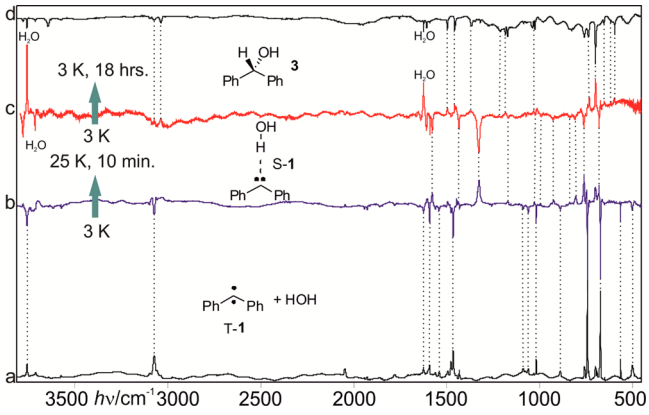

Figure 1. IR spectra showing the formation of the complex S-**1**···H_2O. (a) T-**1** in argon doped with 1% H_2O at 3 K. (b) Difference IR spectrum showing changes after annealing for 10 min at 25 K. Bands pointing downward are disappearing and assigned to T-**1** and H_2O, bands pointing upward are appearing and assigned to the complex S-**1**···H_2O. (c) Difference IR spectrum showing changes after 17 h at 3 K. Bands pointing downward are assigned to the complex S-**1**···H_2O, bands pointing upward are assigned to **3**. (d) **3** matrix isolated in argon at 3 K.

phase and in simulated argon matrices at the QM/MM level of theory (BLYP-D3/def2-TZVP//CHARMM, Figure 2). In the

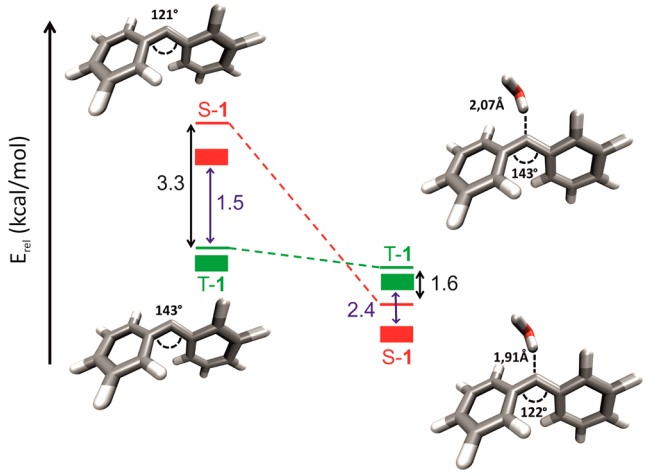

Figure 2. S-T gaps (kcal/mol) of **1** and its most stable complexes with water computed at the BLYP-D3/def2-TZVP level of theory (singlet energies in red, triplet energies in green, all energies including ZPE correction). Values in blue correspond to the QM/MM (BLYP-D3/def2-TZVP//CHARMM) simulations of the system in a box of argon atoms. The red and green boxes represent the range of energies calculated for different matrix sites obtained from several dynamic snapshots.

gas phase, the S-T gap of **1** is calculated to 2.8 kcal/mol (3.3 kcal/mol including ZPE correction) which is close to the 2.9 kcal/mol found in a single point CCSD(T)/cc-pVTZ calculation at the same geometry. In argon, the S-T gap is reduced to 1.5 kcal/mol (QM/MM) which reflects the stronger stabilization of the highly polar S-**1** by solvation with argon compared to the unpolar T-**1**. The S-T gap is inverted by the interaction of the carbene with a single water molecule, with the singlet state predicted to be more stable than the triplet by 1.6 kcal/mol in the gas phase and even by 2.4 kcal/mol in argon.

dx.doi.org/10.1021/ja507894x | J. Am. Chem. Soc. 2014, 136, 15625−15630

The complex S-**1**···H_2O is only metastable and at temperatures between 3 and 12 K rearranges with a rate of $5.8 \pm 0.2 \times 10^{-6}$ to benzhydryl alcohol **3**. In this temperature range, the rearrangement is independent of temperature, which strongly indicates a tunneling reaction. With D_2O a kinetic isotope effect (KIE) of 3 is observed. Compared to the methanol complex,[14] the tunneling rate in the water complex is approximately 1 order of magnitude slower, and the KIE is significantly smaller (KIE = 5 in the methanol complex). This is in accordance with the calculations, which predict an activation barrier for the rearrangement of the water complex of 16.7 kcal/mol (at the BLYP-D3/def2-TZVP level, 14.1 kcal/mol when including ZPE correction, 12.6 kcal/mol for single point CCSD(T)/cc-pVTZ at the same geometry, Figure 3). This barrier is significantly

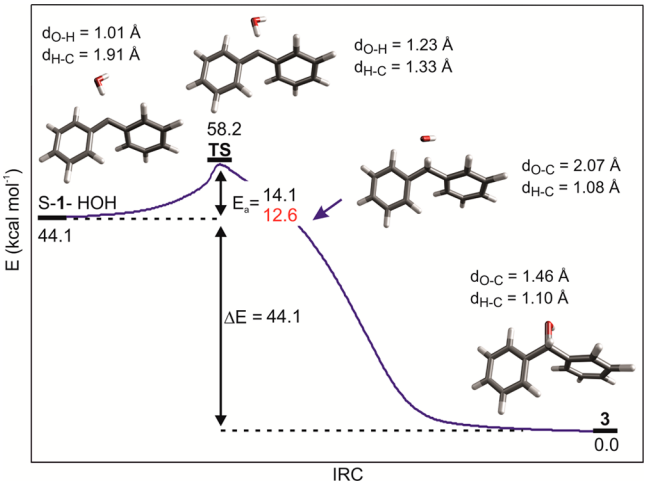

Figure 3. Intrinsic reaction coordinate (IRC) for the rearrangement of the complex S-**1**···H_2O to benzhydryl alcohol **3** calculated at the BLYP-D3/def2-TZVP level of theory. Energies are given in kcal/mol, and the CCSD(T)/cc-pVTZ//BLYP-D3/def2-TZVP calculated activation barrier E_a is shown in red. The structures and some bond distances of S-**1**···H_2O, **3**, and the transition state are shown in the diagram. In addition, a structure along the IRC reminiscent to a contact ion pair between cation **2** and OH^- is presented.

larger than that calculated for the methanol complex. The ion pair **2**···OH^- is neither experimentally observed in the argon matrix nor predicted by theory in the gas phase (Figure 3) to be an intermediate in this rearrangement.

Reaction of DPC in Amorphous Water Ice. It was tempting to use a more polar medium than argon in order to stabilize the **2**···OH^- ion pair. We therefore studied the reaction of **1** in low density amorphous (LDA) water ice.[19] LDA ice is characterized by the absence of long-range periodic structures, and its structure is more similar to liquid water than to crystalline ice. However, while in liquid water hydrogen bonds are exchanged on a ps time scale, LDA ice shows ultraslow reorientation dynamics even at temperatures close to the glass–liquid transition,[20,21] and at 3 K all this motion is expected to be completely frozen.

Diphenyldiazomethane (DPDM) was slowly sublimed and trapped with a large excess of water on a spectroscopic window at 50 K. The LDA ice matrix formed was subsequently cooled to 3 K and photolyzed with visible light (530 nm). During the photolysis, the ice matrix turned intense yellow due to a strong absorption with a maximum at 435 nm. Band position and shape of this band are identical to that reported for the benzhydryl cation **2** (Figure 4).[7,8,11,22,23] The 435 nm absorption is persistent at low temperature and only at

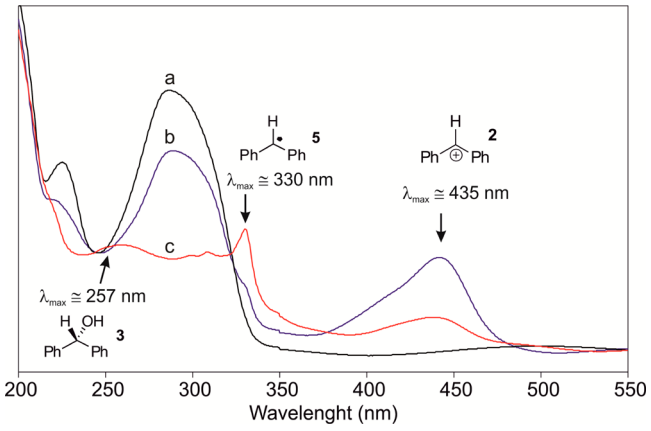

Figure 4. UV–vis spectra showing the photochemistry of DPDM isolated in LDA ice at 8 K. (a) DPDM in LDA ice. (b) 3 h irradiation with λ = 530 nm. The band with λ_{max} = 435 nm is assigned to cation **2**. (c) 10 min irradiation with λ = 450 nm. Bands with λ_{max} = 330 and 257 nm are assigned to radical **5** and alcohol **3**, respectively.

annealing above 40 K slowly disappears. The singlet carbene S-**1** is not observed under these conditions, and the EPR spectrum shows only trace amounts of triplet carbene T-**1** (see Figure S11).

The IR spectrum of cation **2** in LDA ice nicely matches the calculated gas-phase spectrum of **2** (Figure 5). The line-

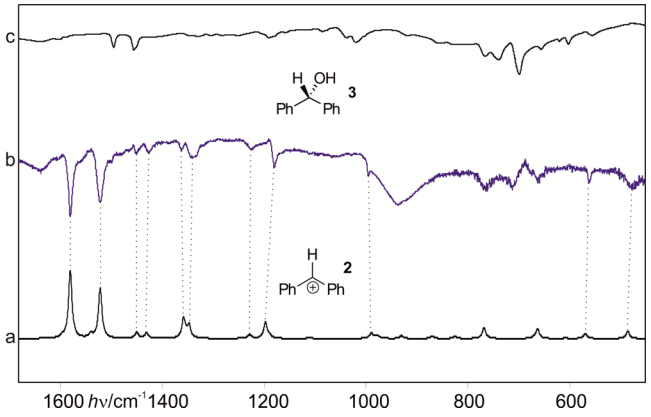

Figure 5. IR spectra in LDA ice showing the reaction of the benzhydryl cation **2** at 100 K. (a) **2** calculated at the BLYP-D3/def2-TZVP level of theory (scaled by 1.007, line width set to approximate experimental spectrum). (b) Difference IR spectrum: bands pointing downward are disappearing upon warming from 3 to 100 K and assigned to **2**. (c) Benzhydryl alcohol **3**, matrix-isolated in LDA ice at 3 K.

broadening in the experimental spectrum is attributed to the inhomogeneity of the matrix cages in LDA ice. To confirm the assignment of the IR bands of **2**, we also generated ^{13}C-**2** with a ^{13}C-labeled cationic center. A strong band at 1522 cm^{-1} exhibits a large ^{13}C isotopic shift of −17.5 cm^{-1} and is assigned to the asymmetric C–C–C stretching vibration across the cationic center. The other absorptions show only small ^{13}C isotopic shifts as predicted by the BLYP-D3 calculations. In D_2O LDA ice, the deuterium transfer to the singlet carbene S-**1** results in the formation of the deuterated carbenium ion d_1-**2**.

dx.doi.org/10.1021/ja507894x | J. Am. Chem. Soc. 2014, 136, 15625–15630

Again, the calculated isotopic shifts are in excellent agreement with the predictions from the BLYP-D3 calculations. Interestingly, ν_{as} C−C−C in d_1-^{12}C-**2** shows almost the same isotopic shift as in ^{13}C-**2**.

To study the interactions between cation **2** and the water matrix, gas-phase calculations of **2** with a cluster of five water molecules were carried out. In addition, QM and QM/MM molecular dynamics simulations (QM MD and QM/MM MD) with **2** and five water molecules as QM region were performed in the gas phase (BLYP-D3/def2-SVP) and in a box of explicit water molecules (BLYP-D3/def2-SVP//CHARMM). Interestingly, cation **2** seems not to form a hydrogen bond with the surrounding water. The C−H stretching vibration at the cationic center is predicted to be a very weak band at 3066 cm^{-1} which is slightly blue-shifted to 3073 cm^{-1} in the presence of five water molecules in the gas phase and to 3071 cm^{-1} in the water box. ν_{as} C−C−C is predicted to show a blue-shift of +6 cm^{-1} by interacting with five water molecules and +9 cm^{-1} in the water box. Thus, there are no specific strong interactions between **2** and the surrounding water, which rationalizes why gas-phase calculations of **2** nicely match the experimental spectra obtained in LDA water ice.

Cation **2** shows an interesting and exceptional photochemistry. Irradiation into the strong visible absorption at 435 nm using a 450 nm LED results in the rapid bleaching of the yellow color of the matrix. A new strong band with a maximum at 330 nm showing a weak vibrational progression is formed concomitantly (Figure 4c), which is assigned to the benzhydryl radical **5** by comparison with literature spectra.[23] The EPR spectrum recorded after the 530 nm photolysis of DPDM in LDA ice deposited on a copper rod shows only traces of DPC T-**1** (Figure S11), unlike the spectrum obtained in solid argon, which shows very intense absorptions of T-**1**. After the 450 nm irradiation, the EPR spectrum shows very intense radical signals, whereas the traces of T-**1** remain almost unchanged. This is in line with the assumption that the EPR silent **2** is the source of the radicals. Due to the line-broadening in LDA ice it is difficult to assign the radical signals, but it is tempting to assume that part of the signal is caused by the benzhydryl radical **5**. The OH radical could not be observed in these experiments.

CONCLUSION

The reaction of carbene **1** with single molecules of water under the conditions of matrix isolation is very similar to the reaction of **1** with methanol: a strongly hydrogen-bonded complex with a singlet ground state is formed (Scheme 1, Figure 1). This gives us the unique opportunity to record IR and UV−vis spectra of the singlet state of diphenylcarbene S-**1**. As expected, the spectra of S-**1** in its water complex are almost identical to that of S-**1** in the methanol complex described by us previously.[14] Both complexes react via quantum chemical tunneling[24,25] to give the products of the formal OH insertion. However, the tunneling of the water complex is about 1 order of magnitude slower, which is in line with the higher activation barrier calculated for the OH insertion in water compared to methanol.

We therefore predict that for carbenes with a S-T gap below 5 kcal/mol, the singlet state should become ground state by hydrogen bonding to water, alcohols, or other molecules with similar hydrogen-bond donor capability. Since S-**1** is stabilized compared to T-**1** even by the weakly solvating argon, we also expect that the stabilization of hydrogen-bonded complexes of carbenes should be even stronger in solvents of higher polarity and polarizability.

In a series of publications, Gudipati et al. have shown that the radical cations of aromatic hydrocarbons are easily obtained by visible light photoionization of the corresponding hydrocarbons in LDA ice.[26−29] Closed-shell cations such as the phenyl, allyl, or benzyl cation could be generated and isolated by ionization of matrix-isolated radicals using vacuum ultraviolet or X-ray irradiation.[30−32] Our experiments establish an alternative route to the isolation of cations in a neutral environment by protonation of carbenes in LDA ice. At temperatures below 40 K, the benzhydryl cation **2** is entirely stable and does not react with the water matrix. The IR spectrum of **2** in LDA ice is nicely matched by gas-phase calculations (Figure 5), indicating only small solvent effects. Obviously, the OH^- produced during the proton transfer from water is stabilized and immobilized in ice enough not to recombine with the cation **2**, despite the high exothermicity of this reaction. It is important to note that **2** in neutral LDA ice is kinetically but not thermodynamically stabilized. The equilibrium in neutral water is very far on the side of benzhydryl alcohol **3**, as indicated by the pK_R^+ value of −13.3. In contrast, in superacidic media carbocations are thermodynamically stable, since the very low pH shifts the equilibria toward the cations. The high reactivity of cation **2** is therefore maintained in LDA ice, which explains the unexpected photochemical electron transfer to produce the benzhydryl radical **5**. In superacidic media we expect radical **5** to be rapidly oxidized to give cation **2**.

In summary, we here describe a novel technique to isolate and kinetically stabilize the highly reactive secondary carbenium ion **2** in a neutral, very clean environment, avoiding superacidic, highly ionic media. This provides easy access to the IR and UV−vis spectra of **2**, and in addition its photochemistry can be investigated without referring to ultrashort time-resolved spectroscopy. The series of experiments described here allow us to synthesize and spectroscopically characterize some of the most important reactive intermediates within the same family of compounds: diphenylcarbene in its triplet ground state T-**1**, the singlet state S-**1** stabilized by hydrogen bonding, the corresponding carbenium ion **2** obtained via proton transfer from water to S-**1**, and finally the radical **5** produced via electron transfer from **2**. This paves the way to explore the chemistry of these species in unprecedented detail.

EXPERIMENTAL SECTION

Preparation of Low Density Amorphous Ice (LDA). Ultrapure water was degassed by successive freeze−thaw and held at room temperature. The water vapors were allowed to co-deposit together with DPDM into a high-vacuum system in different substrates (Cu rod, CsI and sapphire windows, respectively, for EPR, FT-IR, and UV−vis spectroscopy) precooled at 50 K. After finishing the co-deposition the matrices generated were cooled at the lowest temperature possible. The deposition rate of the water vapors was controlled by a fine metering valve.

Matrix Isolation Spectroscopy. Matrix isolation experiments were performed by standard techniques using Sumitomo Heavy industries two-staged closed-cycle helium cryostats (cooling power 1 W at 4 K) to obtain temperatures around 3 K. Water was degassed several times before deposition. The matrices were generated by co-deposition of DPDM and 1% of water with a large excess of argon (Messer Griesheim, 99.99%) on top of different substrates (Cu rod, CsI, and sapphire windows, respectively, for EPR, FT-IR, and UV−vis spectroscopy) cooled at 3 K. A flow rate of approximately 1.80 sccm was used for the deposition of the matrix. Diphenylcarbene T-**1** was generated by photolysis of DPDM at 3 K using a 500 W high-pressure

dx.doi.org/10.1021/ja507894x | J. Am. Chem. Soc. 2014, 136, 15625−15630

mercury lamp and a cutoff filter with 50% transmission at 530 nm. Irradiation at λ = 450 nm was performed by using LED source. After annealing at 25 K for 10 min the matrices were cooled back to 3 K. The experiments in LDA ice matrix were performed in the same manner by replacing the argon with water. FTIR spectra were recorded in the range between 400 and 4000 cm^{-1} with 0.5 cm^{-1} resolution. Matrix EPR spectra were recorded with a Bruker ELEXSYS 500 X-band spectrometer. Matrix UV−vis spectra were recorded with a Varian Cary 5000 UV−vis-NIR spectrophotometer in the range of 200−800 nm with a resolution of 0.1 nm.

Computational Details. All gas-phase DFT geometry optimizations and frequency calculations were carried out using the BLYP functional[33−35] with D3 empirical dispersion correction[36] and the def2-TZVP basis set. The TURBOMOLE program (version 6.4)[37] was employed.

QM MD, QM/MM MD simulations and QM/MM optimizations were performed using the program ChemShell[38,39] as an interface to TURBOMOLE (version 6.4) and CHARMM 31b1.[40] QM MD simulations were conducted at the BLYP-D3/def2-SVP level of theory, while QM/MM MD simulations were carried out at the BLYP-D3/def2-SVP//CHARMM level (10 ps) with a time step of 2 fs under NVT conditions at temperatures of 25 K (Ar simulations), 3 K (gas phase and water simulations), and 200 K (water simulations). The electrostatic interactions were treated using the PME method with a cutoff distance of 1.2 nm.[41] For the QM/MM MD simulations, the molecules of the QM regions (see below) were placed in boxes of argon or water (15 Å box padding). Before the QM/MM MD production runs, the QM atoms were kept frozen, while the MM regions were allowed to move freely for 5 ns under NPT conditions.

A total of 12 QM MD and QM/MM MD simulations of the following systems were performed: (1) QM MD: S-**1**···5H_2O and T-**1**···5H_2O in the gas phase at 3 K; and (2) QM/MM MD: S-**1**, T-**1**, S-**1**···H_2O, and T-**1**···H_2O (QM regions) in a box of explicit Ar at 25 K; S-**1**···H_2O and T-**1**···H_2O (QM regions) in a box of explicit water at 3 K; with S-**1**···5H_2O and T-**1**···5H_2O as QM regions in a water box at 3 K; with S-**1**···5H_2O as QM region in a box of explicit water at 200 K and with benzhydryl cation-**2** as QM region in a box of water at 3 K.

Ten snapshots were taken from each of the MD simulations and reoptimized at the BLYP-D3/def2-TZVP//CHARMM level of theory. Zero-point energies were computed based on harmonic frequency calculations.

■ ASSOCIATED CONTENT

Supporting Information

Synthesis of precursors, extended computational methods, additional spectroscopic data (figures and tables) of the experiments in argon and water matrix, optimized structures of computed compounds. This material is available free of charge via the Internet at http://pubs.acs.org.

■ AUTHOR INFORMATION

Corresponding Authors

wolfram.sander@rub.de
esanchez@kofo.mpg.de

Notes

The authors declare no competing financial interest.

■ ACKNOWLEDGMENTS

This work was supported by the Cluster of Excellence RESOLV (EXC 1069) funded by the Deutsche Forschungsgemeinschaft (DFG). E.S.-G. acknowledges a Liebig Stipend of the Fonds der Chemischen Industrie and the support of the Collaborative Research Center SFB1093 funded by the DFG. We thank Dr. Murthy Gudipati for sharing his expertise in generating amorphous water ice matrices.

■ REFERENCES

(1) Olah, G. A. *J. Org. Chem.* **2001**, *66*, 5943.
(2) Olah, G. A. *Angew. Chem., Int. Ed.* **1973**, *12*, 173.
(3) Phan, T. B.; Breugst, M.; Mayr, H. *Angew. Chem., Int. Ed.* **2006**, *45*, 3869.
(4) Mayr, H.; Ofial, A. R. *Angew. Chem., Int. Ed.* **2006**, *45*, 1844.
(5) Phan, T. B.; Breugst, M.; Mayr, H. *Angew. Chem.* **2006**, *118*, 3954.
(6) Mayr, H.; Ofial, A. R. *Angew. Chem.* **2006**, *118*, 1876.
(7) Peon, J.; Polshakov, D.; Kohler, B. *J. Am. Chem. Soc.* **2002**, *124*, 6428.
(8) Deno, N. C.; Jaruzelski, J. J.; Schriesheim, A. *J. Am. Chem. Soc.* **1955**, *77*, 3044.
(9) Kirmse, W. *Justus Liebigs Ann. Chem.* **1963**, *666*, 9.
(10) Kirmse, W. *Angew. Chem.* **1963**, *75*, 678.
(11) Kirmse, W.; Kilian, J.; Steenken, S. *J. Am. Chem. Soc.* **1990**, *112*, 6399.
(12) Eisenthal, K. B.; Turro, N. J.; Aikawa, M.; Butcher, J. A., Jr.; DuPuy, C.; Hefferon, G.; Hetherington, W.; Korenowski, G. M.; McAuliffe, M. J. *J. Am. Chem. Soc.* **1980**, *102*, 6563.
(13) Eisenthal, K. B.; Moss, R. A.; Turro, N. J. *Science* **1984**, *225*, 1439.
(14) Costa, P.; Sander, W. *Angew. Chem., Int. Ed.* **2014**, *53*, 5122.
(15) Crespo-Otero, R.; Bravo-Rodriguez, K.; Roy, S.; Benighaus, T.; Thiel, W.; Sander, W.; Sanchez-Garcia, E. *ChemPhysChem* **2013**, *14*, 805.
(16) Mardyukov, A.; Sanchez-Garcia, E.; Crespo-Otero, R.; Sander, W. *Angew. Chem., Int. Ed. Engl.* **2009**, *48*, 4804.
(17) Crespo-Otero, R.; Sanchez-Garcia, E.; Suardiaz, R.; Montero, L. A.; Sander, W. *Chem. Phys.* **2008**, *353*, 193.
(18) Sander, W.; Roy, S.; Polyak, I.; Ramirez-Anguita, J. M.; Sanchez-Garcia, E. *J. Am. Chem. Soc.* **2012**, *134*, 8222.
(19) Tulk, C. A.; Benmore, C. J.; Urquidi, J.; Klug, D. D.; Neuefeind, J.; Tomberli, B.; Egelstaff, P. A. *Science* **2002**, *297*, 1320.
(20) Shalit, A.; Perakis, F.; Hamm, P. *J. Phys. Chem. B* **2013**, *117*, 15512.
(21) Low, F.; Amann-Winkel, K.; Loerting, T.; Fujara, F.; Geil, B. *Phys. Chem. Chem. Phys.* **2013**, *15*, 9308.
(22) Ammer, J.; Sailer, C. F.; Riedle, E.; Mayr, H. *J. Am. Chem. Soc.* **2012**, *134*, 11481.
(23) Sailer, C. F.; Thallmair, S.; Fingerhut, B. P.; Nolte, C.; Ammer, J.; Mayr, H.; Pugliesi, I.; de Vivie-Riedle, R.; Riedle, E. *ChemPhysChem* **2013**, *14*, 1423.
(24) Ley, D.; Gerbig, D.; Schreiner, P. R. *Org. Biomol. Chem.* **2012**, *10*, 3781.
(25) McMahon, R. J. *Science* **2003**, *299*, 833.
(26) Gudipati, M. S. *J. Phys. Chem. A* **2004**, *108*, 4412.
(27) Gudipati, M. S.; Allamandola, L. J. *Astrophys. J.* **2004**, *615*, L177.
(28) Gudipati, M. S.; Allamandola, L. J. *J. Phys. Chem. A* **2006**, *110*, 9020.
(29) Gudipati, M. S.; Allamandola, L. J. *Astrophys. J.* **2006**, *638*, 286.
(30) Winkler, M.; Sander, W. *Angew. Chem., Int. Ed.* **2000**, *39*, 2014.
(31) Winkler, M.; Sander, W. *J. Org. Chem.* **2006**, *71*, 6357.
(32) Misic, V.; Piech, K.; Bally, T. *J. Am. Chem. Soc.* **2013**, *135*, 8625.
(33) Becke, A. D. *Phys. Rev. A* **1988**, *38*, 3098.
(34) Lee, C.; Yang, W.; Parr, R. G. *Phys. Rev. B* **1988**, *37*, 785.
(35) Miehlich, B.; Savin, A.; Stoll, H.; Preuss, H. *Chem. Phys. Lett.* **1989**, *157*, 200.
(36) Grimme, S.; Antony, J.; Ehrlich, S.; Krieg, H. *J. Chem. Phys.* **2010**, *132*, 154104.
(37) Ahlrichs, R.; Bär, M.; Häser, M.; Horn, H.; Kölmel, C. *Chem. Phys. Lett.* **1989**, *162*, 165.
(38) *Chemshell, a Computational Chemistry Shell* (www.chemshell.org).
(39) Sherwood, P.; de Vries, A. H.; Guest, M. F.; Schreckenbach, G.; Catlow, C. R. A.; French, S. A.; Sokol, A. A.; Bromley, S. T.; Thiel, W.; Turner, A. J.; Billeter, S.; Terstegen, F.; Thiel, S.; Kendrick, J.; Rogers, S. C.; Casci, J.; Watson, M.; King, F.; Karlsen, E.; Sjovoll, M.; Fahmi, A.; Schafer, A.; Lennartz, C. *J. Mol. Struct. THEOCHEM* **2003**, *632*, 1.

(40) Brooks, B. R.; Brooks, C. L., III; Mackerell, A. D., Jr.; Nilsson, L.; Petrella, R. J.; Roux, B.; Won, Y.; Archontis, G.; Bartels, C.; Boresch, S.; Caflisch, A.; Caves, L.; Cui, Q.; Dinner, A. R.; Feig, M.; Fischer, S.; Gao, J.; Hodoscek, M.; Im, W.; Kuczera, K.; Lazaridis, T.; Ma, J.; Ovchinnikov, V.; Paci, E.; Pastor, R. W.; Post, C. B.; Pu, J. Z.; Schaefer, M.; Tidor, B.; Venable, R. M.; Woodcock, H. L.; Wu, X.; Yang, W.; York, D. M.; Karplus, M. *J. Comput. Chem.* **2009**, *30*, 1545.
(41) Essmann, U.; Perera, L.; Berkowitz, M. L.; Darden, T.; Lee, H.; Pedersen, L. G. *J. Chem. Phys.* **1995**, *103*, 8577.